AFRL-AFOSR-JP-TR-2018-0030

Doppler-free velocimetry in hypersonic flow

Sean OByrne
University of New South Wales-NEW NCAGE Code

04/09/2018
Final Report

Air Force Research Laboratory
AF Office Of Scientific Research (AFOSR)/ IOA
Arlington, Virginia 22203
Air Force Materiel Command

REPORT DOCUMENTATION PAGE

Form Approved
OMB No. 0704-0188

1. REPORT DATE *(DD-MM-YYYY)*	2. REPORT TYPE	3. DATES COVERED *(From - To)*
09-04-2018	Final	15 Jun 2016 to 14 Dec 2017

4. TITLE AND SUBTITLE
Doppler-free velocimetry in hypersonic flow

5a. CONTRACT NUMBER

5b. GRANT NUMBER
FA2386-16-1-4028

5c. PROGRAM ELEMENT NUMBER
61102F

6. AUTHOR(S)
Sean OByrne

5d. PROJECT NUMBER

5e. TASK NUMBER

5f. WORK UNIT NUMBER

7. PERFORMING ORGANIZATION NAME(S) AND ADDRESS(ES)
University of New South Wales-NEW NCAGE Code
HIGH STREET
KENSINGTON, NSW, 2052 AU

8. PERFORMING ORGANIZATION REPORT NUMBER

9. SPONSORING/MONITORING AGENCY NAME(S) AND ADDRESS(ES)
AOARD
UNIT 45002
APO AP 96338-5002

10. SPONSOR/MONITOR'S ACRONYM(S)
AFRL/AFOSR IOA

11. SPONSOR/MONITOR'S REPORT NUMBER(S)
AFRL-AFOSR-JP-TR-2018-0030

12. DISTRIBUTION/AVAILABILITY STATEMENT
A DISTRIBUTION UNLIMITED: PB Public Release

13. SUPPLEMENTARY NOTES

14. ABSTRACT
The PI final report describes the development of a Doppler-Free velocimetry technique for use in low-density plasmas and hypersonic facility flows. In the report, the PI describes implementation of a novel Doppler-Free spectroscopy setup that uses a retroreflected counter-propagating beam that is separated from the incoming beam by polarization. The PI has also developed a plasma cell within a converging/diverging nozzle to provide a calibrated argon plasma with a known flow velocity. The system has been assembled and tested in a static rubidium cell, and in flowing argon gas. The viability of seeding a hypersonic flow with a rubidium salt has also been tested. The PI has had good success under this grant and will present the work during the International Symposium on Rarefied Gas Dynamics in 2016.

15. SUBJECT TERMS
hypersonic, velocity measurement, laser diagnostic, AOARD, saturated absorption spectroscopy

16. SECURITY CLASSIFICATION OF:			17. LIMITATION OF ABSTRACT	18. NUMBER OF PAGES	19a. NAME OF RESPONSIBLE PERSON
a. REPORT	b. ABSTRACT	c. THIS PAGE			SINGLETON, BRIANA
Unclassified	Unclassified	Unclassified	SAR	21	19b. TELEPHONE NUMBER *(Include area code)* 315-227-7007

Standard Form 298 (Rev. 8/98)
Prescribed by ANSI Std. Z39.18

AOARD Final Report - Doppler-Free Velocimetry in Hypersonic Flow

Sean O'Byrne, Suzanne Sheehe, Tremayne Kaseman

March, 2018

1 Report Data

Report Type: Final Technical Report
Primary contact email: T.Callaghan@unsw.edu.au
Primary contact phone: +61 (2) 9385 6193
Institution Name: The University of New South Wales
Grant Title: Doppler-Free Velocimetry
Grant Number: FA2386-16-1-4028
PI Name: A/Professor Sean O'Byrne
Program Officer: Dr Jermont Chen
Reporting Period Start Date: June 14, 2016
Reporting Period End Date: December 14, 2017

Report Abstract:

This Report outlines work done on the development of a Doppler-Free velocimetry technique for use in low-density plasmas and hypersonic facility flows. To test the technique, we have implemented a novel Doppler-Free spectroscopy setup that uses a retroreflected counter-propagating beam that is separated from the incoming beam by polarization. We have also developed a plasma cell within a converging/diverging nozzle to provide a calibrated argon plasma with a known flow velocity. The system has been assembled and tested in a static rubidium cell, and in flowing argon gas. The viability of seeding a hypersonic flow with a rubidium salt has been tested.

Archival publications published during reporting period:

The Rb shearing interferometry has been published in the proceedings of the International Symposium on Rarefied Gas Dynamics in 2016. The Ar plasma results will be presented at the International Symposium on Rarefied Gas Dynamics in July, 2018.

Change In Research Objectives:

Initially, it was not clear whether a rubidium-seeded flame or a plasma would be used for the calibration of the system. Preliminary modelling indicated that an atmospheric pressure flame would require too high a laser power to achieve saturation. Instead we have used a low-pressure static Rb cell for initial measurements. Also, we changed from the original proposed fiber-based design to a free-space design because of the difficulty of alignment and ensuring constant polarization direction in all the fibers. The free-space system was much simpler to set up.

2 Introduction

This report presents work on the use of saturation spectroscopy to measure velocity in low-density plasmas and hypersonic flows. We have implemented a free-space saturation spectroscopy system that uses a single retroreflected beam to carry the saturation signal, making it suitable for applications where tunable diode laser absorption spectroscopy (TDLAS) is used. The system has two significant advantages compared to TDLAS for low-density gases:

1. It uses atomic absorption lines, and atomic absorption lines have stronger absorption linestrengths than the molecular species typically used for these applications.

2. The use of saturation spectroscopy has a built-in zero-velocity wavelength reference in the spectrum.

The use of rubidium in atom optics and in wavelength locking configurations has meant that Rb external cavity diode lasers (ECDLs) and distributed Bragg reflector (DBR) diode lasers with very good (MHz) spectral resolution can be conveniently sourced. The ECDLs in particular have extremely narrow linewidths, allowing very precise zero-velocity calibration to be built into the acquired spectrum.

The high spectral resolution makes this technique more sensitive to Doppler shifts at low flow velocities than standard TDLAS. We have two applications where such a capability is desirable: process flows in plasma applications such as physical vapor deposition and regions of low flow speed in hypersonic facilities. We have performed experiments in Ar for the low-speed case and are investigating the feasibility of measurements at high speeds in impulsive hypersonic facilities.

2.1 Physical Principle of Saturated Absorption

Even while at rest, the atoms and/or molecules in a sample of gas are in constant random motion, with a probability distribution that is dependent on the temperature, determined by a Maxwell-Boltzmann distribution. As each atom or molecule has a different velocity, the absorption spectrum will be Doppler shifted from the zero-velocity frequency ν_0 according to

$$\nu_D = \nu_0 \left(1 + \frac{v}{c}\right) \tag{1}$$

Although the natural linewidth of the transition is very narrow, the fact that each molecule or atom experiences a different Doppler shift has the effect of broadening the absorption feature. The dependence of the full-width at half-maximum of the absorption linewidth on temperature is given by

$$\Delta\nu_D = \frac{2\nu_0}{c}\sqrt{\frac{2k_B T}{M}\ln(2)} \tag{2}$$

where k_B is the Boltzmann constant, M is the atomic mass of the atom and T is the gas temperature.

While this Doppler broadening can be useful as a way of measuring gas temperature, it limits the resolution of Doppler-shift bulk velocity measurements, as the ability to determine the bulk velocity depends on the ratio of the Doppler shift to the width. As temperatures become higher, and for low bulk velocities, the increased Doppler width makes it more difficult to determine the change in peak location due to bulk velocity of the gas, presenting a fundamental limit for standard absorption measurements.

Doppler-free spectroscopy, or saturated absorption spectroscopy, is a technique first developed by Hänsch and co-workers [1] for the investigation of the fine and hyperfine structure of atomic spectra. The hyperfine splitting in particular is obscured by the Doppler broadening mentioned above, and the Doppler-free technique is used to select a specific velocity subgroup of molecules. The Doppler-free technique is similar to standard scanning absorption spectroscopy, but instead of passing a single laser beam through the gas and measuring the absorption of the light, the Doppler-free method uses two nearly counterpropagating laser beams: one a low-power probe beam and the other a higher-power pump beam. The basic schematic is shown in Figure 1 When the pump beam passes through the gas it

promotes a particular group of the atoms or molecules in the gas that have been Doppler shifted to the laser frequency into an excited state. If the laser is sufficiently powerful, it can promote a significant fraction of the population to the excited state.

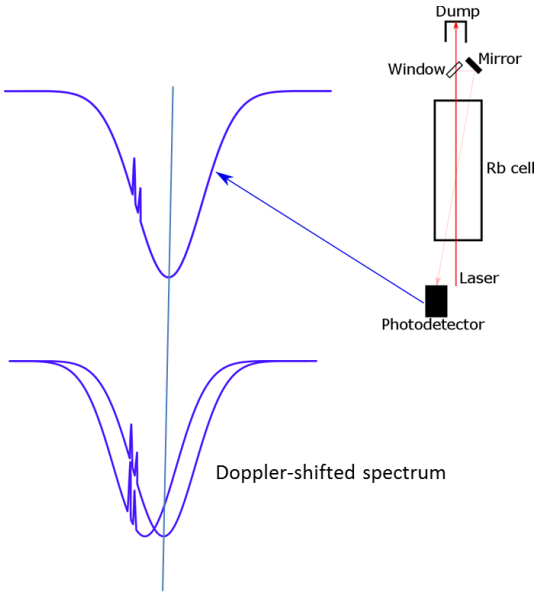

Figure 1: Doppler-free absorption principle

The weaker nearly counter-propagating laser beam is typically at the same wavelength as the pump beam. If the atoms or molecules in the gas sample are in motion, then the probe beam will excite atoms or molecules with the negative of the velocity that the forward-propagating beam has excited. These are different atoms to those excited by the pump beam for every velocity group except those with zero velocity in the laboratory reference frame. In this case, for these zero-velocity atoms or molecules, both lasers are exciting the same group of particles. The pump laser depletes the lower-state atoms or molecules, which reduces the population available for excitation by the counter-propagating probe beam. This manifests as a dip in the absorption spectrum at the transition frequency of the zero-velocity atoms. Because only one velocity group is excited, the dip in the absorption profile is much narrower than the Doppler-broadened lineshape, and has a width determined by the convolution of the natural linewidth and the linewidth of the exciting laser.

This behaviour provides a marker for the zero-velocity location of the transition. Because the dip always occurs only for those atoms or molecules with zero velocity, it marks the transition frequency regardless of the bulk velocity of the gas. If the gas is in motion, then the Doppler-broadened absorption line will be blue- or red-shifted but the saturation dips will not move, as shown in Figure 1. This provides a very accurate zero-velocity reference for the Doppler-shift measurement, allowing a simple and high-precision method for measurement of low flow velocities. This is particularly important in low-density, low-velocity flows such as process plasmas for surface coatings and for embedded regions of low-speed flows in hypersonic flows.

2.2 Previous use as a Diagnostic Technique

While there have been many studies of Doppler-free absorption in the context of determination of fine and hyperfine structure of atomic line spectra, there have been fewer attempts to use saturated absorption as a flow diagnostic technique. Typically absorption spectroscopy has been performed with molecular species without the use of saturated absorption, using techniques like tunable diode laser absorption spectroscopy (TDLAS) [2]. However, there are several applications, such as measurements in discharge flows for physical vapour deposition processes and high-enthalpy hypersonic flows, where atomic species are readily available and where velocity measurements are important. For the inves-

tigation of these flows, atomic absorption transitions have several desirable features. First, they are typically much stronger that molecular transitions, allowing simple and fast direct absorption measurements to be used rather than more complex methods like wavelength modulation detection [3] or balanced ratiometric detection [4]. Second, atomic species have isolated transitions that are easier to interpret than the often complex spectra due to molecular species. Finally, atomic transitions survive at higher temperatures than molecular transitions that are subject to dissociation at temperatures in excess of 3000 K. Because of their strength, atomic lines are easily saturated at moderate laser powers, making saturated spectroscopy measurements at low pressure available using relatively inexpensive and highly spectrally resolved diode laser sources such as external cavity diode lasers, distributed feedback lasers, distributed Bragg reflector lasers and vertical cavity surface-emitting lasers.

The first study that used saturated absorption for flow diagnostic purposes was that of Goldsmith [5], using perpendicular crossed beams to provide a spatially resolved saturated absorption spectrum. This was not a Doppler-free measurement because the beams are not co-propagating, but the measurement was spatially resolved because it is made in the region where the two crossed beams overlap. This paper provided the first proof of concept that sodium seeded into an atmospheric pressure hydrogen/oxygen flame could be used to produce spatially resolved saturated absorption spectra. No diagnostic measurements were presented, however. Kychakoff et al. [6] used this method to measure OH concentration in a laminar flame. Zizak et al. [7] implemented a similar system using a single laser for measurements of OH in a methane-air flame.

The first application of the saturated absorption measurement in supersonic flow was performed by Phillips and Perram [8], who measured temperature in a supersonic nozzle flow using saturated absorption of iodine, for investigation of the behaviour of a chemical oxygen iodine laser. This method used a cross-beam intermodulated detection technique to determine the translational temperature from the iodine fluorescence, in a spatially resolved manner. By co-propagating the two beams, the interaction region overlapped with all velocity groups, providing a full Doppler-broadened signal from the interaction region. Fitting of the width of this profile allowed the translational temperature to be determined, although the measurement was complicated by the complex structure of the molecular iodine spectrum.

None of these measurements were used to determine velocity, and all of them involved the use of either CW or pulsed dye lasers, or a combination of the two. This makes such systems bulky and expensive to implement. Aramaki et al. [9] used a combination of laser induced fluorescence and saturated absorption spectroscopy to measure spatially resolved velocities in an argon plasma. The saturation spectroscopy measurement was used to provide a zero-velocity wavelength reference against which the PLIF signal could be calibrated. These measurements were performed using an external cavity diode laser, operating at 696 nm. The use of fluorescence detection limits the temporal resolution achievable with a method like this. For this reason, in our experiments we concentrate on the use of saturation absorption spectroscopy alone, which can be achieved at high scan rates using fast photodetectors and current-scanned diode lasers.

More recently Nomura and Komurasaki [10] implemented the cross-beam saturated absorption measurement of Goldsmith [5] to measure translational temperature in an arc-heated low-density argon wind tunnel facility. The measurement system used an external cavity diode laser operating at 772 nm.

Of all the papers mentioned here, only one, that of Aramaki et al., has been used to measure velocity. The work presented here is a first attempt to use saturated absorption spectroscopy of a diode laser to measure velocity using the Doppler-free Lamb dip as a zero-velocity wavelength reference.

2.3 Spectroscopy of Rb and Ar

There is a fortunate overlap in wavelength between the $5^2s_{1/2} \leftarrow 5^2p_{3/2}$ and the $5^2s_{1/2} \leftarrow 5^2p_{1/2}$ fine structure transitions of Rb and the transition between the 3p5(2P°1/2) 4s and 3p5(2P°3/2) 4p levels of Ar, both of which occur around 795 nm. For this reason, a wavelength of 795 nm has been chosen for both sets of experiments, allowing the same optical arrangement to be used for both species, providing a platform that can investigate either argon plasmas or Rb-seeded hypersonic flows.

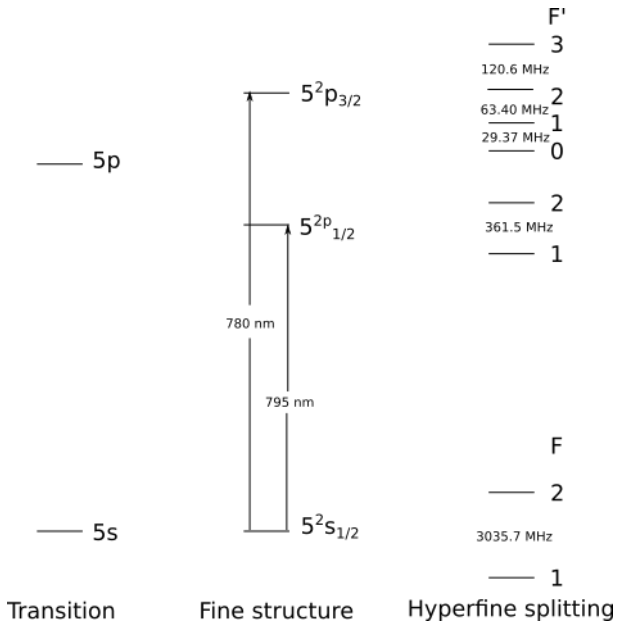

Figure 2: ^{85}Rb Energy level diagram showing fine and hyperfine splitting.

Rubidium has two main stable isotopes ^{85}Rb and ^{87}Rb, which have abundances of 72.2 and 27.8 per cent respectively. Figure 2 shows the spectroscopic structure of the rubidium 85 D lines near 780 and 795 nm. These lines are very strong outer-shell electronic transitions between the 5s and 5p levels of the rubidium atom. In common with other alkali metals such as sodium and lithium, rubidium has very strong D-line transitions. The fine structure splits these lines into two main lines, the 795-nm line being labelled D1 and the slightly stronger 780 nm line labelled D2. These lines are further split into several hyperfine levels, as shown in the rightmost energy level diagram in Figure 2. The frequency differences here are smaller than the Doppler width of the atom, meaning that the structures are hidden by the Doppler broadening. Rubidium is a good atomic species to work with because as well as having very strong transitions that are easily saturated, it is relatively heavy for an atomic species. As can be seen from Equation 2, the Doppler width scales as the inverse square root of molecular weight, so heavier species will tend to have narrower linewidths and hence better shift-to-width ratios than lighter species. As an indication, at room temperature Rb has a Doppler width of 506 MHz compared to atomic hydrogen, which has a width of 5.35 GHz. Argon has a room-temperature Doppler width of 740 MHz.

In addition to the well understood Rb D1 line at 795 nm, there is an absorption line for a metastable state of argon at approximately the same wavelength, allowing the same laser system to be used for both species. The argon transition has been used in diode laser absorption spectroscopy studies of pulsed nanosecond-duration discharges in argon [11], being used to measure temperature and concentration histories in these plasmas, and has also been used in saturation fluorescence velocity measurements in high-speed flow by Aramaki et al [9].

The spectral data for the Rb transitions has been taken from the comprehensive study of Steck [12] for both the 87 and 85 isotopes of rubidium.

3 Apparatus and Method

3.1 ***Plasma Apparatus***

For Doppler-free absorption measurements, the choice of excitation laser is very important. The laser needs to have very narrow line width, and needs to be tunable over the entire width of a Doppler-broadened transition. For some applications it may also necessary to tune the laser very quickly.

For the above reasons, most recent work in Doppler-free absorption studies has concentrated on

the use of external cavity diode lasers (ECDLs) as the light source. These lasers combine a number of desirable properties, being relatively high powered, very narrow linewidth and relatively quick to scan over a transition. The particular laser we chose for this work was a MOGLabs CatEye ECDL, with a MOGLabs wavelength meter for determining the wavelength of the laser throughout the experiment. This laser has a very narrow nominal linewidth of the order of 100 kHz. In comparison, a single mode DFB laser has a spectral width of 1–2 MHz, or a vertical cavity surface emitting laser which has a width in excess of 30 MHz.

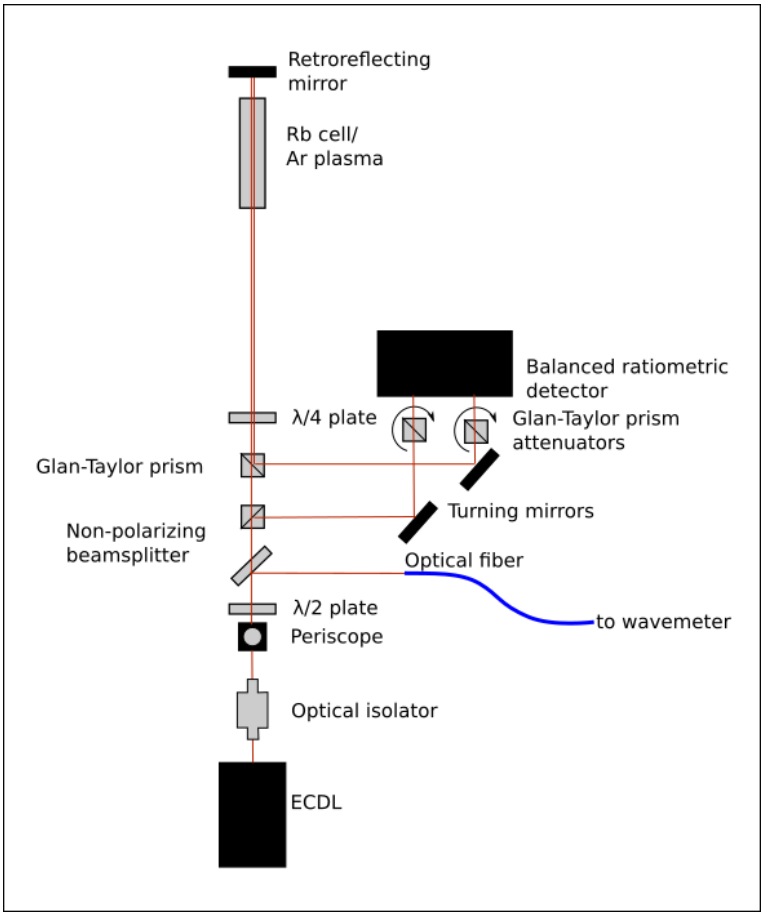

Figure 3: Doppler-free absorption spectroscopy apparatus.

The optical arrangement for the experiments is shown in Figure 3. This is somewhat different to the generic Doppler-free system shown in Figure 1. In this apparatus, the two beams are made to overlap throughout the flow (not just in a single overlap region). In this way, there is no difference, other than the direction of the Doppler shift, between the flow experienced by the pump and the probe beams. The two beams are separated from one another by a series of wave plates and Glan-Taylor polarizing prisms. Upon leaving the laser, the beam passes through an optical isolator to prevent feedback from back reflections. The laser beam is then raised to the height of the cell using a periscope arrangement. The linearly polarized beam from the laser then passes through a half-wave plate where its polarization plane can be adjusted. A glass slide removes a small fraction of light to a wavelength meter, and a second polarization independent beamsplitter that is used to provide a reference signal.

The beam's polarization is controlled by rotating the half-wave plate until throughput through the Glan-Taylor prism was maximized. The beam then passes through a quarter-wave plate which makes the polarization circular, hits a mirror that reverses the direction of the circularly polarized light, and then is transformed into a linear polarization that is orthogonal to the original direction once it passes through the quarter-wave plate on the return trip through the system. This orthogonally polarized light is redirected perpendicularly by the Glan-Taylor prism. The signal and reference beams are then

passed through a further two Glan-Taylor prisms, which act as variable attenuators before the beams pass to a balanced ratiometric detector [4]. This autobalancing detector returns an output signal that is proportional to the absorbance in the cell. Although the figure shows the two beams perfectly superposed, we used a very small angular separation between the two beams, allowing control over the degree of overlap between the two beams within the region of plasma and minimizing the adverse effect of propagation of the back-reflected beam into the ECDL.

Initially the system was set up using polarization maintaining optical fibers and collimators. It was found that the difficulty with coupling light into fibers once it had passed through the flow and the difficulty associated with controlling the polarization of the beam made it difficult to set up the system, whereas the free-space system is reasonably robust and very simple to implement.

In addition to the optical system, it was necessary to find a source of plasma whose velocity could be relatively easily varied, and which would be uniform. The device that we used to make these velocity measurements is shown in cross-section in Fig. 4 (a). The cell is designed to be a converging-diverging subsonic nozzle with a pair of flat-plate electrodes at the throat. By controlling the pressure differential across this nozzle, the speed of the flow through the throat can be determined.

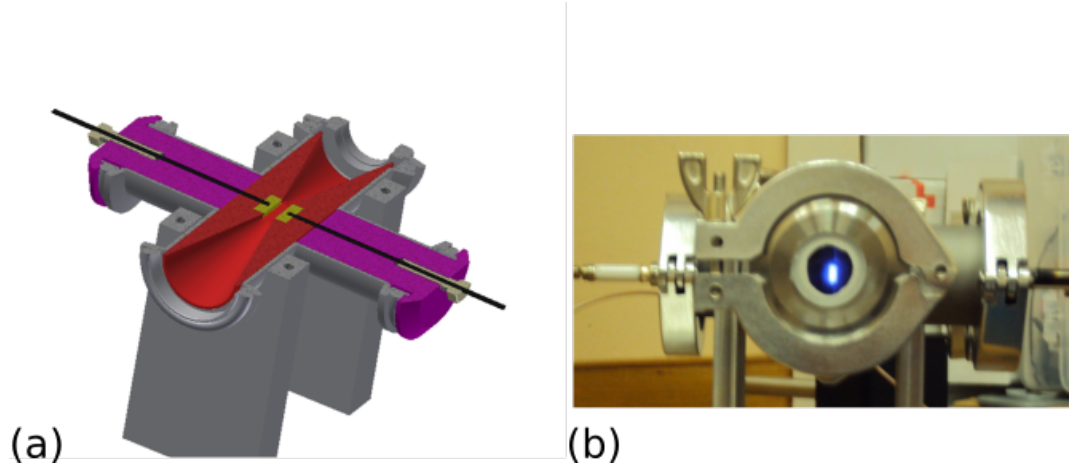

Figure 4: Argon plasma velocimetry cell (a) diagram (b) emission image.

The flat plate electrodes ensure a uniformly distrubuted discharge provided the pressure is maintained throughout. The plasma was powered by a 600V DC discharge at a pressure differential of between 1 and 15 Torr. The power supply, a SRS PS350 high-voltage DC power supply, was used to create the discharge. The power supply has a maximum supply current of 5 mA, but for these experiments was limited to 3 mA, for reasons that will be explained in the discussion of results. Figure 4 (b) shows the glow arising from this particular configuration.

3.2 Tunnel Experiments

While we had initially planned to perform Rb saturated absorption experiments in the T-ADFA shock tunnel, we were not able to complete these parts of the experiments because of a hardware failure. Prior to this we conducted two direct absorption experiments in the shock tunnel, which are described and the results presented in the document.

The tunnel conditions used for these tests were Condition E of the T-ADFA facility. The nominal flow conditions for Condition E are given in Table 1. Previous work used a 1.5-mm-thick unscored diaphragm. For these tests, we used a 2-mm-thick diaphragm indented with a cross using a 12-tonne press, to minimize the debris resulting from the diaphragm burst process. The indentation was chosen to produce the same burst pressure in hydraulic testing as the unscored diaphragm. The tunnel used a conical nozzle with a 0.5-inch diameter throat and a 12 inch diameter exit.

The experiments involved measurements at the nozzle exit of the T-ADFA facility. The optical arrangement for the experiments is shown in Fig. 5.

Table 1: T-ADFA Condition E nominal flow parameters

Parameter	Value
Nozzle reservoir burst pressure (MPa)	43.1
Diaphragm thickness (mm)	2.0
Shock speed (m/s)	1915
Nozzle reservoir pressure (MPa)	10.5
Total temperature (K)	3050
Total enthalpy (MJ/kg)	3.8
Nozzle exit speed (test time) (m/s)	2514
Nozzle exit temperature (K)	156

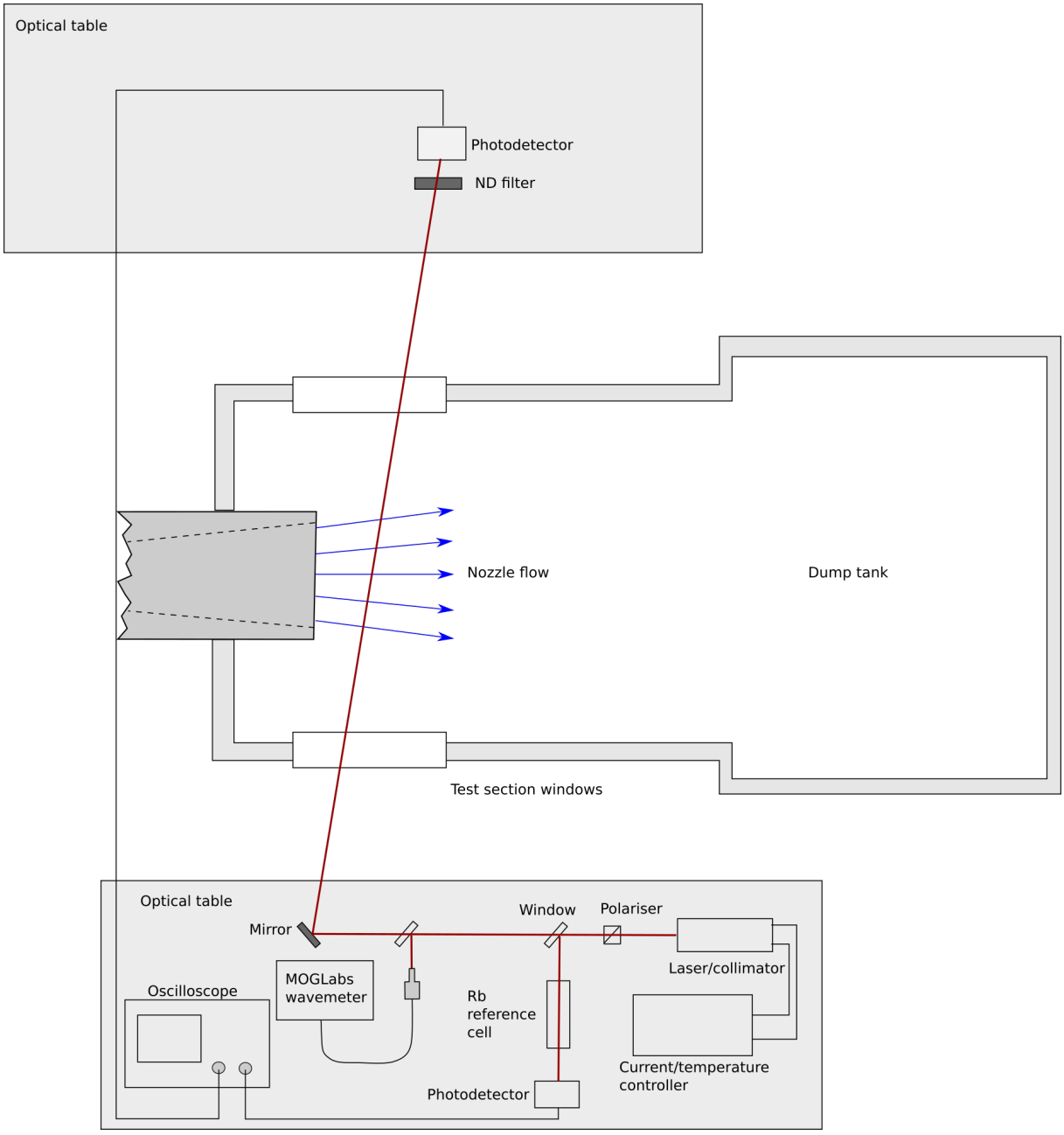

Figure 5: Tunnel experiment arrangement

The laser used for the test was a Photodigm distributed Bragg Reflector (DBR) laser operating at 795 nm, with a maximum output power of 120 mJ. This laser was chosen because, unlike the external cavity diode lasers used for the plasma experiments, it could be current scanned over a limited wavelength range at kHz scan rates. As the shock tunnel has an effective time of only 1-2 milliseconds, a laser source has to be able to perform several wavelength scans over that time in order to produce a time-resolved spectrum, and these scan rates cannot be achieved with a piezo-tuned ECDL. Previous studies in our group [11] have used vertical cavity surface emitting lasers (VCSELs) to scan across similar wavelength ranges at very high rates with very good spectral resolution, but the low power of single-mode VCSELs makes them poorly suited to saturation spectroscopy. Although DBR lasers are susceptible to mode hopping, their combination of high power, relatively fast scan rates and narrow linewidth make them a good choice for these applications. The laser was driven by an ILX LDC-3744C combined temperature and current controller modulated by an SRS DS340 signal generator.

The laser was passed through a Glan-Taylor prism to allow the light intensity to be controlled through polarisation. The light then passed a wedged fused silica window through a rubidium reference cell, maintained at a constant 40.0 degrees Celcius, which provided a zero-velocity reference absorption spectrum, measured using a Thorlabs DET100 biased silicon photodiode. The photodiode supply was terminated with 4.4 kOhms, providing sufficient time resolution to scan at 5 kHz and sufficient signal intensity to be measured on an oscilloscope. A second wedged fused silica window picked off a small portion of the beam intensity and redirected it via optical fiber to a MOGLabs wavemeter calibrated between 780 and 813 nm for an accurate measurement of the laser wavelength. The remainder of the light was passed at an angle through the test section of the shock tunnel to a neutral density filter and a second DET100 detector on the other side of the tunnel. As the windows had limited diameter, the laser beam could only be traversed for these experiments at an angle of 6.16 $^\circ$ from perpendicular to the flow. The beam diameter for these experiments was around 3 mm, which was larger than the 1 mm by 1 mm square area of the photodetector. This made the beam less susceptible to variations caused by beam steering than would have occurred for a narrower beam.

For these experiments, the seed species used was rubidium chloride (RbCl). A saturated solution of the salt was made and was applied to the end-wall of the shock tunnel, so that when the shock wave reflects from the surface the Rb atoms are released and travel down the hypersonic nozzle with the main flow. The use of a salt is necessary for rubidium because of the very high reactivity of the metal. The salt is quite unreactive, and can be applied very evenly as a solution to the interior of the tunnel.

The signals from the two photodiodes were collected by a LeCroy HDO6104 digital storage oscilloscope operating in single-shot mode. The direct absorption method was used to determine the absorbance for both the tunnel and reference cell beams simultaneously. The laser was scanned at 5000 Hz for these measurements. Tests in the cell at different scan rates showed that the distortion of the spectrum due to the response time of the detection system was not significant at these conditions.

4 Results

4.1 ***Resonantly Enhanced Shearing Interferometry in Rubidium***

In order to use Doppler-Free absorption spectroscopy in a shock tunnel, rubidium must be seeded into the flow, as it is not a naturally occurring atomic species in air. When we first developed this technique using the lithium D1 line [13], we seeded the flow by using a foil of metallic lithium at the end of the shock tube. When the shock wave reflects from the end of the tube, the Li metal is readily vaporized in metallic form and high concentrations of Li vapor atoms can be generated in this way. However, if rubidium is to be used for this purpose, the metal is too reactive to safely use as metallic sheets. Instead, for Rb, we considered the use of ionic Rb salts, as these are chemically very stable, but can be easily dissolved, allowing the salts to be spread evenly over the secondary diaphragm and shock tube end-wall of the T-ADFA facility.

Figure 6 shows a RESI image for a hypersonic leading edge configuration characterized by very low density and relatively small density gradients. Images without the Rb show only the forebody shock

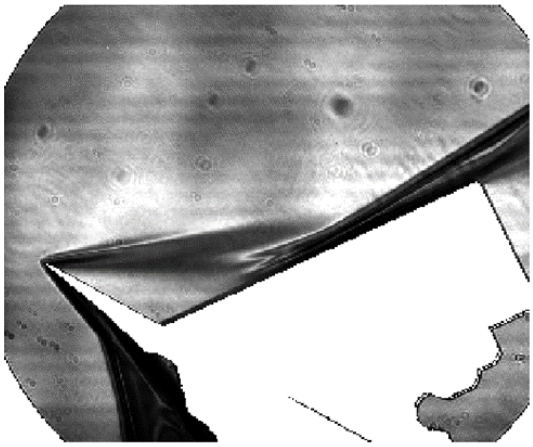

Figure 6: RESI image of a separated flow using the Rb D2 transition, from [14]

wave, as the system is not sufficiently sensitive to density gradients in this flow field. Although not nearly as strong an effect as the effect for metallic lithium seeding, there is sufficient Rb in the flow at high enthalpy to allow a relatively straightforward way of seeing the shock tunnel flow. This indicates that it should be feasible to make absorption measurements using rubidium in a hypersonic shock tunnel flow.

4.2 Doppler-Free Absorption in a Static Rubidium Vapor Cell

A static gas cell containing rubidium vapor was used for the first Doppler-free spectroscopy measurements. This was used because the spectroscopy of the hyperfine structure of rubidium is well understood, and the tunnel tests were planned to use rubidium as the absorbing species. Initial measurements were made with no physical overlap between the pump and probe beams, resulting in a standard absorption spectrum. Figure 7 is an example spectrum, obtained by scanning the laser over a 10 GHz spectral region. This is sufficient to see every major line in the D1 doublet.

It is clear from Figure 7 that all 4 of the major peaks are visible, but that the hyperfine structure cannot be seen under the Doppler broadening. Although the x-axis in the figure is time, the full span of the scan corresponds to a scan of 10 GHz. The FWHM of the absorption features is about the predicted 500 MHz value.

By overlapping the two beams from the retroreflecting mirror, we are able to produce the saturation peaks as dips in the Doppler-broadened absorption profile, as shown in Figure 8. Although the general shape of the features is the same as that for the direct absorption measurement, the hyperfine peaks are apparent in the image. The number of these peaks is determined by the hyperfine splitting of the transitions. Some of the stronger lines have several hyperfine levels apparent. In the figure, we have labelled the more important of the transitions. For the velocimetry measurements we would prefer to have a transition that contains only one hyperfine level. The $^{87}\mathrm{Rb}^{5}S_{1/2}, F = 1 -^{5} P_{1/2}, F = 1$ transition is a good candidate. This transition has a lower strength than the others but is much simpler to use in a velocimetry measurements than the stronger lines on the spectral scan, which have more Doppler-free lines and therefore a more complex structure.

4.3 Doppler-Free Absorption in an Argon Plasma

Initially the argon plasma was set up for high-voltage operation, but as soon as the discharge was struck, the resistance of the plasma would drop to a point that exceeded the maximum output current of the supply and would trigger the protective circuit breaker of the supply. A 10 kOhm 5 Watt resistor was placed in series with the supply to reduce the maximum current, but even then the circuit breaker would regularly switch. If the current output of the supply was limited to 3 mA, the DC plasma could

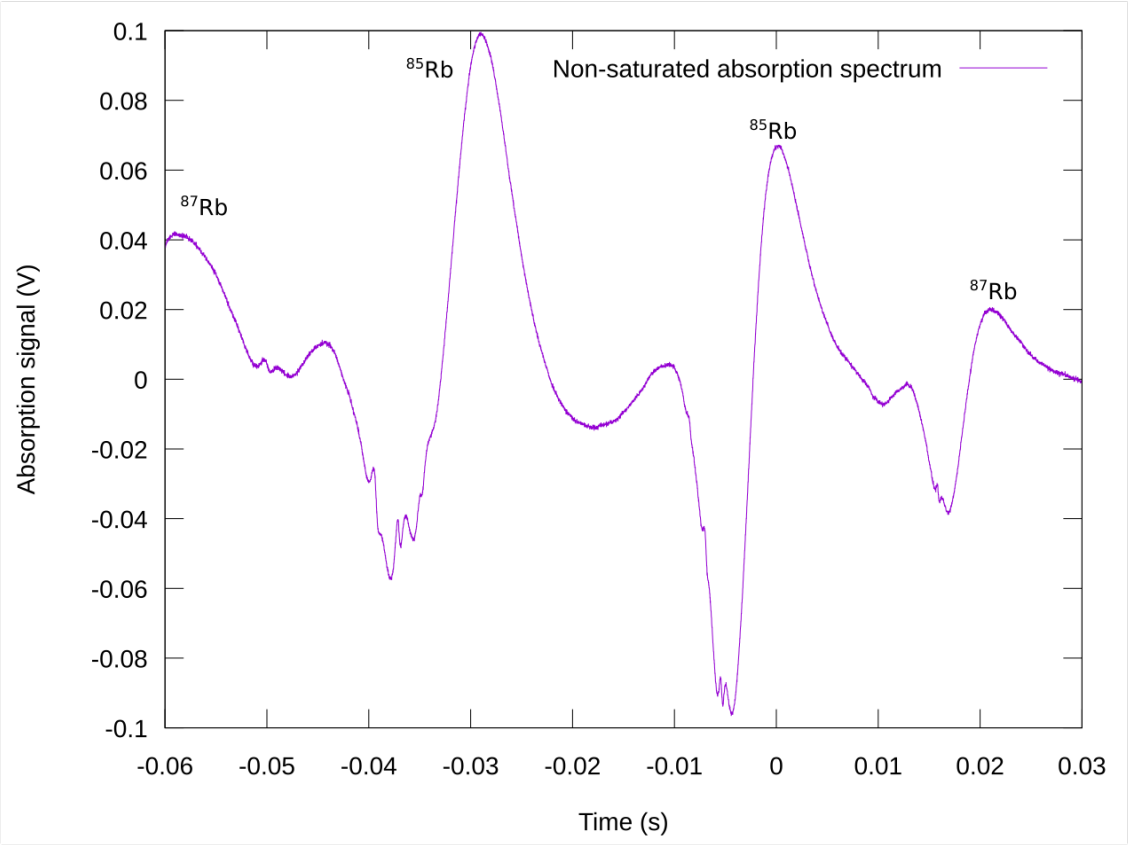

Figure 7: Absorption spectrum of Rb D1 lines

be maintained statically at pressures up to 10-15 Torr without triggering the circuit breaker.

The first experiments performed involved measurement of a DC discharge under constant pressure static gas conditions. Under these conditions, while it was possible to sustain a glow discharge, there was no apparent absorption from the metastable state transition at 794.98 nm. Even using a sensitive log-ratio detection system that we have used with absorbances below 10^{-4} we were not able to find a convincing absorption signal in the static cell. Previous studies of nanosecond discharges using these transitions [11] showed that it was possible to get strong signals with direct absorption. In those cases, however, the voltages and currents were higher than those obtained in these experiments and therefore the population of the metastable lower level of the transition was probably much greater than in the case of this DC discharge, leading to more absorption signal.

It was only when a pressure differential was imposed upon the flow that an absorption line could be discerned. The line was clearly due to the excited argon in the plasma because it would disappear from the spectrum when the electrical discharge was removed. The non-saturated absorption spectrum is shown in Fig. 9. This plot was obtained when a pressure difference of 7 Torr was maintained across the converging-diverging nozzle, with a current limit of 3 mA and a voltage of 289 V maintained between the two electrodes. The pressure differential (7 Torr to 0.1 Torr) is sufficient to allow sonic flow in the throat region of the nozzle.

The absorption signal was weak, but strong enough to be seen using log-ratio detection using a New Focus Nirvana autobalancing log-ratio detector. The transition seemed to have some structure to it, which was unexpected as no structure had been seen when the transition had been used on previous plasma investigations, appearing as a single Gaussian lines. There may have been some structure induced by the Doppler shift caused by the flow through the converging/diverging nozzle under the pressure differential.

The frequency scale on the x-axis was estimated by measurements at the extreme values of the wave-

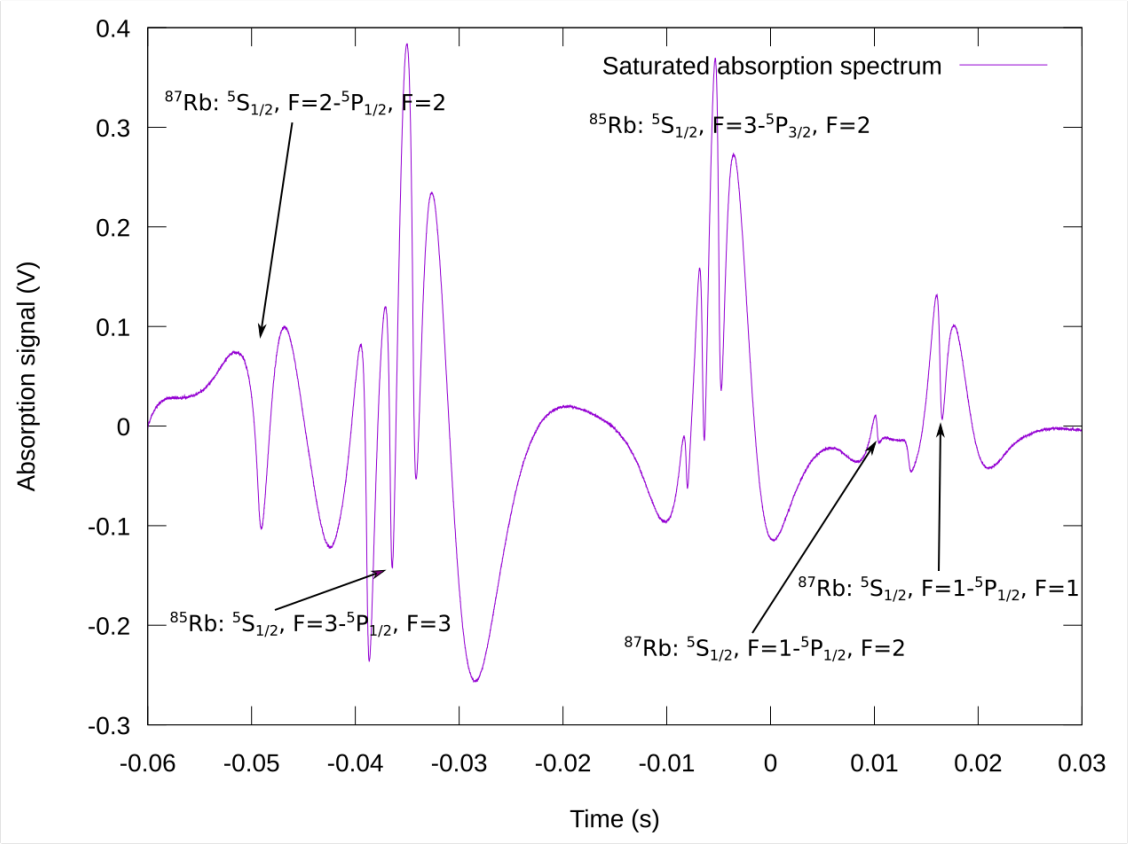

Figure 8: Doppler-free absorption spectrum of Rb D1 lines

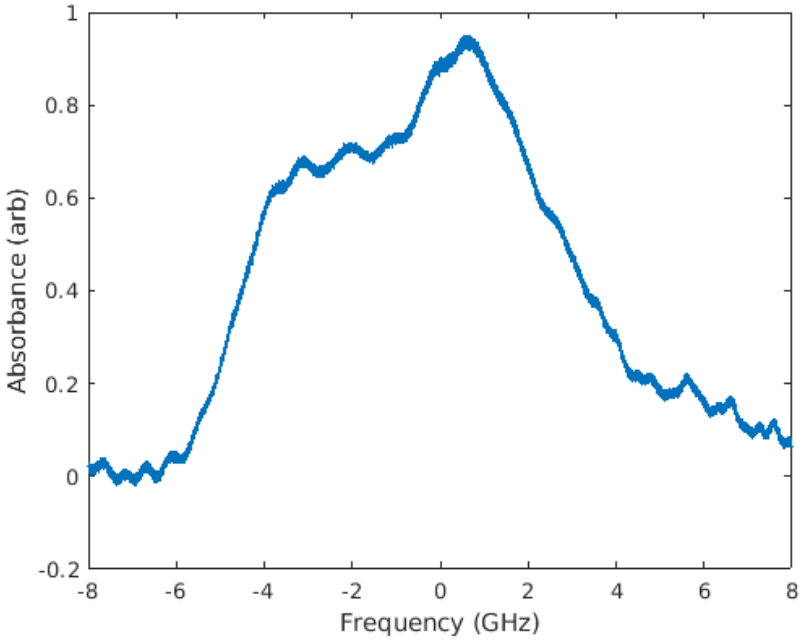

Figure 9: Argon non-saturated absorption spectrum.

length scan obtained using the MOGLabs wavelength meter, and is roughly consistent with the expected Doppler width of the argon transition at 400K. The y-axis units are arbitrary, but are proportional to the absorbance. In addition to the two-peak shape of the transition, there is some modulation of the absorption signal caused by etaloning in the optical system. While wedged windows were used on the gas cell, the cube beamsplitter used to separate the reference and signal beams may have encouraged the formation of these etalons.

When set up in Doppler-free operation, as per Fig. 3, the signal was quite weak and the etalon effect was more pronounced. Fig. 10 shows the spectrum obtained in this configuration, with a Lamb dip apparent in the spectrum. The etaloning is very apparent in this measurement as a sinusoidal modulation in the absorption spectrum. Again, the signal on the y-axis is presented in arbitrary units, but is proportional to the absorbance.

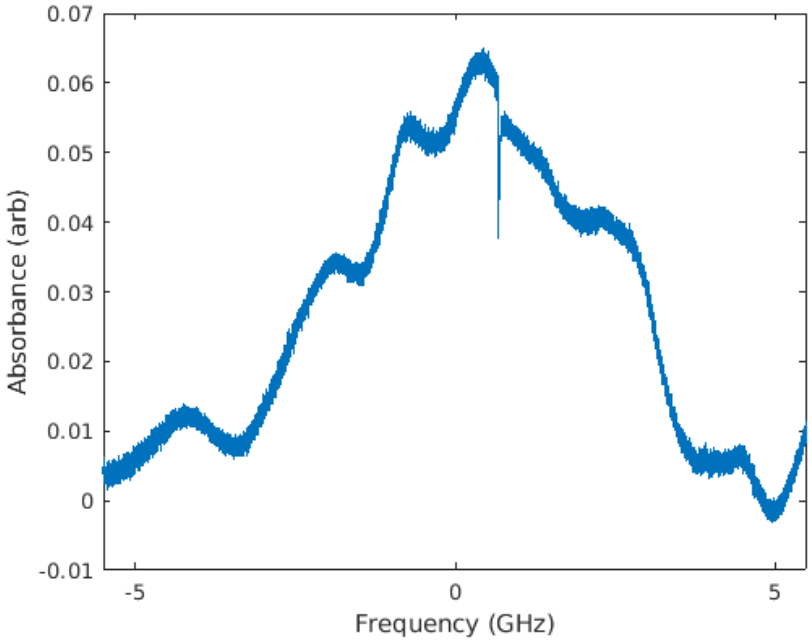

Figure 10: Argon saturated absorption spectrum.

As for the non-saturated absorption measurement, it was not possible to make the absorption measurement when the gas in the cell was static, and only when a pressure differential existed was there a strong enough signal to see. This means that we were unable to determine a Doppler shift directly as we had no zero-velocity reference for the argon plasma.

4.4 Tunnel Experiments

Figure 11 shows the raw reference and tunnel absorption signals as a function of time after the reflection of the shock wave in the tunnel. There is a disturbance in the signal very soon after reflection, perhaps because of stress waves caused by the shock reflection process passing through the optical system. There is then a delay for 16 scans before the beam passing through the tunnel shows as an absorption signal. The fact that the beam passing through the tunnel is still intensity-modulated during this time and the reference cell beam shows absorption means that there is no obvious Rb absorption signal, although as we will see shortly there is a very small amount of rubidium absorption occurring at this time.

On the 17th spectrum after shock reflection, at around 3.3 ms in Fig. 11, or around 2.5 ms after shock reflection, absorption suddenly becomes apparent, and this signal continues until the 31st scan at 6.1 ms after shock reflection, when the absorption becomes much stronger. This sudden change in absorption

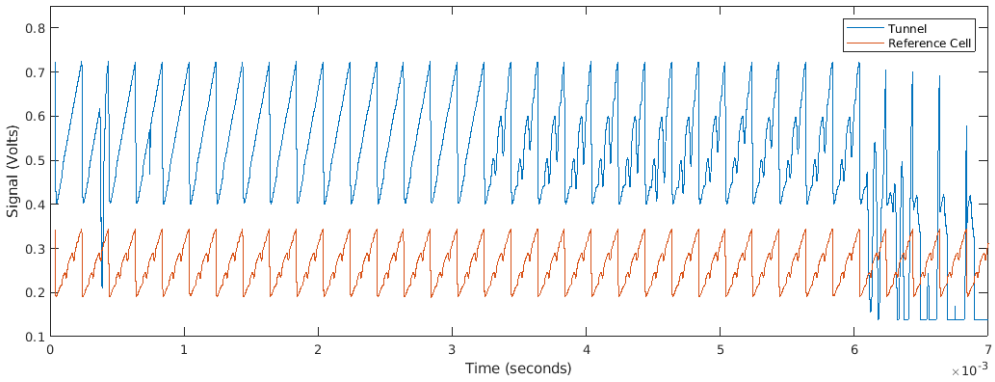

Figure 11: Scans of tunnel absorption spectra

may indicate the arrival of the hot driver gas, which may liberate much more Rb vapor than the air flow during the test time, although in the absence of an independent measure of driver gas arrival, it is difficult to be certain.

During the time between 2.5 and 5.4 ms after shock reflection, the absorbance in the tunnel is around 3 times greater than that within the cell. The width of the lines are similar in both cases, although one would expect the temperature in the tunnel flow to be lower than in the room-temperature gas cell. The anomalous extra width may be due to the Doppler shift of the light due to the expansion of the nozzle flow creating velocity components parallel and antiparallel to the laser beam direction. The range of Doppler shift has the effect of making the absorption signal look broader than it would be with a perfectly uniform freestream flow.

The raw absorption data in Fig. 11 can be calibrated to provide Doppler shift information by knowing from Fig. 2 that the separation between the two large ^{85}Rb D1 peaks is 3.035 GHz. Taking the isolated F_g = 2 peak as a reference detuning of 0 GHz, the time axis can be converted into a frequency axis. This allows the Doppler shift of the isolated line to be converted directly to a velocity component in the direction of the laser beam, and from there to a freestream velocity measurement using the 83.84 degree angle between the laser beam and the nozzle flow.

After fitting the time data to frequency by calibrating against the known spacing between the two main peaks in the reference cell, the backgrounds to the direct absorption spectra were fit for three regions outside the influence of the lines, using a third-order polynomial, and this background-fitted data was used as a reference for the calculation of the absorbance. An example spectrum obtained some 3 ms after the shock reflection, is shown in Fig. 12. In this figure, the red curve represents the absorption trace in the static Rb cell, while the blue curve shows the absorption spectrum for the tunnel nozzle flow. The blue curve is noticeably Doppler shifted away from the spectrum in the cell. The signal-to-noise ratio of the tunnel data is very high, particularly when compared with previous tunnel data acquired in the same facility for molecular water vapor [15]. The small oscillations near the peak of the red curve are from etalons generated in the static rubidium vapor cell. The angle of the beam through the test section windows prevented etalons being generated by those windows. This plot is typical of the comparison between the tunnel and reference spectra during the test time. The greatest height of the peak in the tunnel flow varied from 0.15 to 0.3 during the steady flow time, but the relative heights of the two ^{85}Rb peaks always remained constant.

Measuring the reference cell spectrum full-width at half-maximum (FWHM) provides a measured FWHM in the room temperature cell of 580 MHz. The calculated FWHM of the cell at 298K is 506 MHz. The discrepancy may be with the calibration to the frequency shift between the two peaks. Although the temperature in the freestream, based upon Table 1 is predicted to be lower than room temperature, the spectrum is clearly more broad than that of the reference cell. The reason for this difference is that the nozzle flow is expanding and the absorption spectrum will be Doppler-shifted both to the blue and the red ends of the spectrum as the laser beam passes through the nozzle flow. This has the effect of

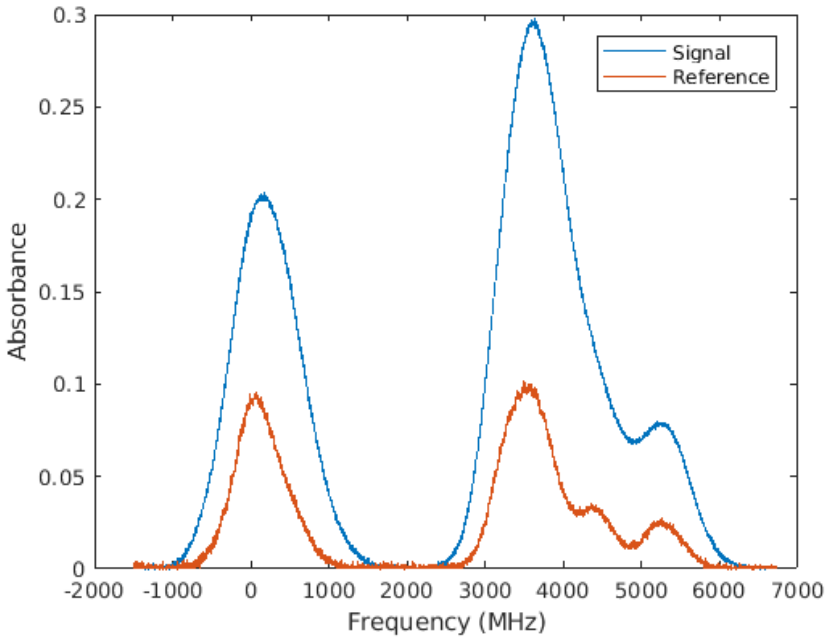

Figure 12: Tunnel and cell absorbance spectra

broadening the absorption profile. This is an unavoidable outcome of the path-integrated nature of the absorption measurement. Although the Doppler-shifting due to the expansion of the nozzle flow will broaden the spectrum, it should not change the location of the peak, which is used to measure the Doppler shift of the bulk flow, as the radial velocity distribution that broadens the profile is symmetrical with respect to the laser beam path.

Figure 13 is a comparison of the absorbances from the cell and the tunnel, normalized to the peak intensity of the isolated peak. This plot was obtained 1.0 ms after shock reflection, during the nominal test time of the flow. Although the signal from the nozzle flow is much weaker than that in the rubidium cell, and the signal-to-noise ratio in the spectrum is only around 3 to 1, there is clearly still structure in the spectrum corresponding to a Doppler-shifted rubidium absorption profile.

Figure 14 shows the nozzle reservoir transducer pressure trace for the tunnel run where the absorption data in Fig. 11 was obtained. It is clear that for this condition, the steady flow time is approximately 1 ms long, if the steady time is defined as the time before the pressure has reduced to 90 per cent of the initial pressure. The fact that the first visible absorption scans are occurring some 2.5 ms after shock reflection indicates that the Rb is only being released into the flow significantly after the nominal test time of the facility at this total enthalpy of 3.8 MJ/kg.

Therefore we conclude from this experiment that although there is rubidium in the flow during the test time, there is less signal than required to make a direct absorption measurement of the Doppler shift. It may be necessary to use a more sensitive detection method, such as difference amplification, at these conditions. There seems to be an induction time in the facility before sufficient Rb is generated to be easily seen in direct absorption. It would be reasonable to expect that this induction time should become shorter as the total enthalpy of the flow condition increases.

1. Determination of Velocity

   We can determine the velocity using the measured Doppler shift in two ways by assuming either the full-width-at half-maximum (FWHM) of the room-temperature rubidium spectrum or the separation between the two large peaks in the spectrum (3.035 GHz) are known. We used the latter calibration for the experiments. Doppler shifts and velocities calculated referenced to the width of the profile in the reference cell would be lower by 15 per cent than those presented here.

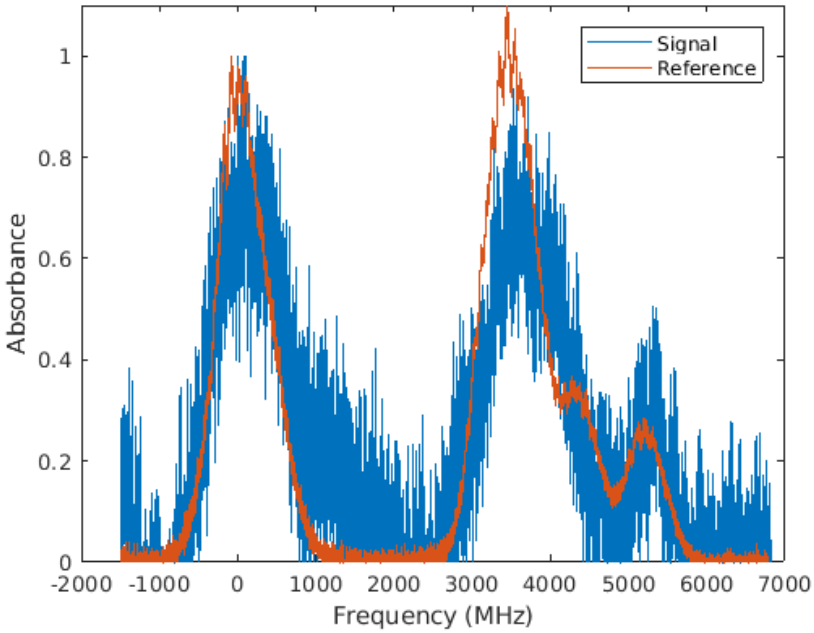

Figure 13: Tunnel and cell absorbance spectra

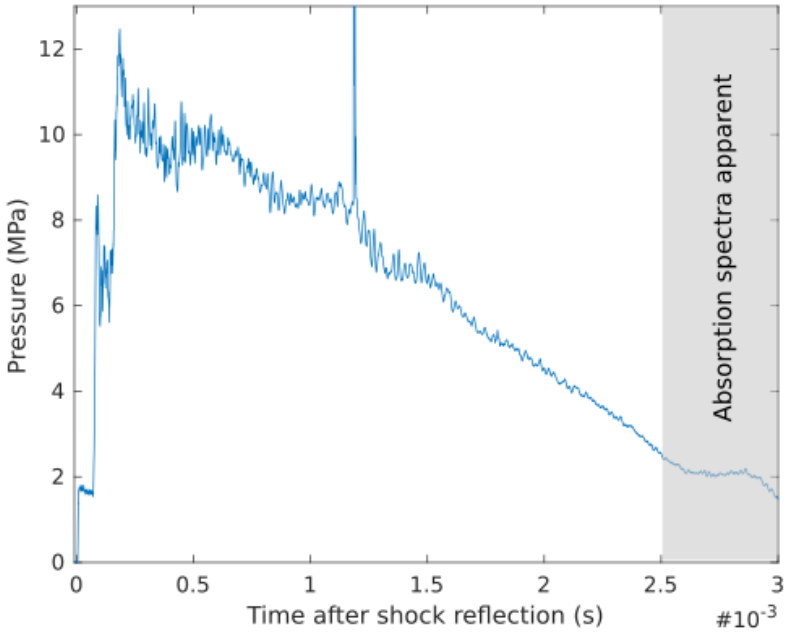

Figure 14: Nozzle reservoir pressure trace for Rb absorption measurements.

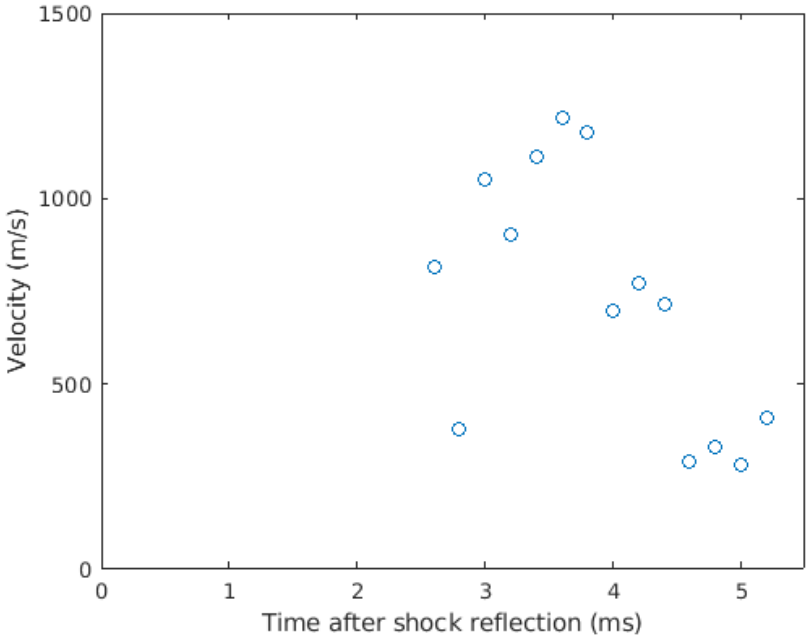

Figure 15: Nozzle exit velocity measurements

The velocity measured in the freestream as a function of time is presented in Fig. 15. Only those spectra where the rubidium signal had good signal-to-noise ratio were fitted, which corresponds to those spectra obtained between 2.6 and 5.4 ms after shock reflection. The velocities reduced from a maximum of around 1000-1200 m/s to around 300 m/s before the absorbance became too large to get a good velocity measurement. Apart from one anomalously low measurement at 2.8 ms after shock reflection, there is a generally decreasing trend in velocity with time. The velocities are significantly lower than the nominal exit velocity in Table 1, but this is because we are making measurements at the very end of the flow time, where the flow velocities are expected to decrease. In each of the points plotted in Fig. 15, the velocities were well defined and easy to measure from the plots.

5 Outcomes

In this project we have achieved the following objectives:

- We have developed a novel retroreflected configuration for making precise Doppler-free absorption measurements.
- We have designed and constructed a plasma test facility capable of producing a calibrated flow of electrically excited argon gas, for validation of the technique.
- We have designed and implemented an optical system that uses retroreflection to provide the Doppler-free signal, separating the two beams using changes in polarization. This method has a few advantages over the standard way of measuring shown in Figure 1, as both beams travel through the same region of space and the absorption and saturation occur throughout the flowfield. The setup has been successfully tested in both a static Rb cell and an argon plasma.
- We have identified transitions at 795 nm for both argon and rubidium that allow the same laser source to be used to investigate both shock tunnel flow and low-pressure argon plasma flows.

- We have implemented Doppler-free absorption measurements in a small argon plasma nozzle facility, using a DC discharge. Although the absorption signal is very low, the saturation-induced Lamb dip can be seen. For these experiments we were unable to obtain a zero-velocity reference signal, so were not able to use the system in its current form as an absolute velocity measurement system. Because of the closeness of the Rb line and the Ar line, it should be possible to reference the velocity to the saturated absorption in a Rb reference cell, and use the inferred known location of the unshifted argon transition signal to achieve an absolute velocity measurement. We are currently investigating this method for measurements in the plasma.

- We have implemented the first scanning Rb absorption system in a free-piston shock tunnel facility, using seeded Rb atoms vaporized from the walls of the shock tunnel during the shock reflection process. At the low total enthalpy conditions chosen here, there was a significant delay between the start of the tunnel's operation and the first clear signal from the absorption system, although there is some absorption signal during the test time. This delay is most likely due to the finite time required to vaporize the flow. This delay time is likely to reduce significantly at higher total enthalpy conditions, where the total temperature of the gas is significantly higher than the dissociation temperature of RbCl. A second strong increase in the absorption signal occurs around 5.4 ms after shock reflection, most likely due to the arrival of hot driver gas at the nozzle reservoir, although it is difficult to be sure from this data.

- We have shown that the use of a simple absorption system and a reference static Rb cell allows for a measurement of the velocity in a hypersonic flow with a higher signal-to-noise ratio than measurement systems using molecular species such as water vapor. The use of Rb also removes the need for either placing pitch and catch optics and electronics within the test section of the facility, as unlike the case for water vapor, there is no Rb absorption outside the nozzle flow. The Rb signal was also very constant when the signal could be found, so the salt seeding seemed to provide a uniform seeding level for some of the flow. The sudden increase in absorption signal at around 6 ms after shock reflection is attributed to the sudden increase in temperature upon the arrival of the argon driver gas, but may also be due to a sudden increase in the Rb vapor content due to another cause. The biggest potential barrier to the adoption of the technique to lower total enthalpy flows is this delay in the onset of Rb absorption. For the flow condition investigated here, the onset of Rb absorption occurred after the steady-pressure test time was finished in the facility.

There is still work remaining to be done in the application of Doppler-free absorption spectroscopy in the shock tunnel. The results with direct absorption presented here are promising, and at these low density flow conditions, there is a very good chance that saturated absorption can be measured. A replacement laser has been purchased, and the final Doppler-free experiments will be continued using a saturated absorption system in place of the direct simple absorption system presented in this report. However even without the Doppler-free reference, this method provides some high-quality absorption data that can be used to make time-resolved velocity measurements in shock tunnels.

References

[1] A Siegel, JE Lawler, B Couillaud, and TW Hansch. Doppler-free spectroscopy in a hollow-cathode discharge: Isotope-shift measurements in molybdenum. *Physical Review A*, 23(5):2457, 1981.

[2] Mark G Allen. Diode laser absorption sensors for gas-dynamic and combustion flows. *Measurement Science and technology*, 9(4):545, 1998.

[3] Gregory B Rieker, Jay B Jeffries, and Ronald K Hanson. Calibration-free wavelength-modulation spectroscopy for measurements of gas temperature and concentration in harsh environments. *Applied optics*, 48(29):5546–5560, 2009.

[4] Philip CD Hobbs. Ultrasensitive laser measurements without tears. *Applied optics*, 36(4):903–920, 1997.

[5] JEM Goldsmith. Spatially resolved saturated absorption spectroscopy in flames. *Optics letters*, 6(11):525–527, 1981.

[6] George Kychakoff, Robert D Howe, and Ronald K Hanson. Spatially resolved combustion measurements using cross-beam saturated absorption spectroscopy. *Applied optics*, 23(9):1303–1305, 1984.

[7] Giorgio Zizak, Francesco Cignoli, and Sergio Benecchi. Spatially resolved saturated absorption measurements of oh in methane-air flames. *Applied optics*, 26(19):4293–4297, 1987.

[8] Grady T Phillips and Glen P Perram. Crossed-beam intermodulated fluorescence spectroscopy as a spatially resolved temperature diagnostic for supersonic nozzles. *Applied optics*, 48(26):4917–4921, 2009.

[9] Mitsutoshi Aramaki, Kohei Ogiwara, Shuzo Etoh, Shinji Yoshimura, and Masayoshi Y Tanaka. High resolution laser induced fluorescence doppler velocimetry utilizing saturated absorption spectroscopy. *Review of Scientific Instruments*, 80(5):053505, 2009.

[10] Satoshi Nomura and Kimiya Komurasaki. Translational temperature measurements in a shock layer by point-measurement laser absorption spectroscopy. *Journal of Thermophysics and Heat Transfer*, 29(4):649–652, 2015.

[11] Rounak Manoharan, Toby K Boyson, and Sean O'Byrne. Time-resolved temperature and number density measurements in a repetitively pulsed nanosecond-duration discharge. *Physics of Plasmas*, 23(12):123527, 2016.

[12] Daniel A Steck. Rubidium 87 d line data, 2001.

[13] Robert Hruschka, Sean O'Byrne, and Harald Kleine. Diode-laser-based near-resonantly enhanced flow visualization in shock tunnels. *Applied optics*, 47(24):4352–4360, 2008.

[14] T. P. Kaseman. *Optical studies of leading-edge separation in high-enthalpy, low-density hypersonic flows*. PhD thesis, School of Engineering and IT, UNSW Canberra, 2017.

[15] Yedhu Krishna, Suzanne L Sheehe, and Sean B O'Byrne. A time-resolved temperature measurement system for free-piston shock tunnels. In *31st AIAA Aerodynamic Measurement Technology and Ground Testing Conference*, page 2249, 2015.